Journal of *Marine Science and Engineering*

MDPI

Article

Effectiveness of Staggered Pile Arrangements for Managing River Mouth Closures on Gravel Beaches

Yamato Torii [1], Masami Kiku [2,*], Norimi Mizutani [3] and Tomoaki Nakamura [3]

[1] Advanced Course for Interdisciplinary Technology Development, National Institute of Technology, Gifu College, 2236-2 Kamimakuwa, Motosu 501-0495, Japan
[2] Department of Civil Engineering, National Institute of Technology, Gifu College, 2236-2 Kamimakuwa, Motosu 501-0495, Japan
[3] Department of Civil and Environmental Engineering, Nagoya University, Nagoya 464-8603, Japan; mizutani@civil.nagoya-u.ac.jp (N.M.); tnakamura@nagoya-u.jp (T.N.)
* Correspondence: kiku@gifu-nct.ac.jp; Tel.: +81-58-320-1324

Abstract: Several small- and medium-sized rivers connecting to the Shichiri-Mihama coast are closed due to debris. The progression of river mouth closures increases the risk of flooding in the watershed, so countermeasures are necessary. In this study, piles were installed in a staggered pattern to prevent river mouth closures. The hydraulic model experiment was conducted to assess how countermeasure (staggered piles) installation affects topographic change under various wave conditions. The installation of the staggered piles was found to be effective in moving the location of the berm forward more than 10 cm offshore and reducing gravel accumulation by up to 57%. The effect of the staggered piles is particularly significant in wave conditions with small wave gradients. The pile row spacing should be short to maintain the complexity of the staggered arrangement. The effects of changes in the flow velocity field and differences in the bottom sediment should also be considered for practical use. Eventually, the installation of the staggered piles will be expected to prevent the long-term development of berms, thus preventing estuary closure.

Keywords: 3D topographic measurement method; countermeasure; estuary closure; topographic change; continuous piles; hydraulic model experiment; gravel beach

check for updates

Academic Editor: Ahmed Benamar

Received: 6 January 2025
Revised: 27 January 2025
Accepted: 28 January 2025
Published: 29 January 2025

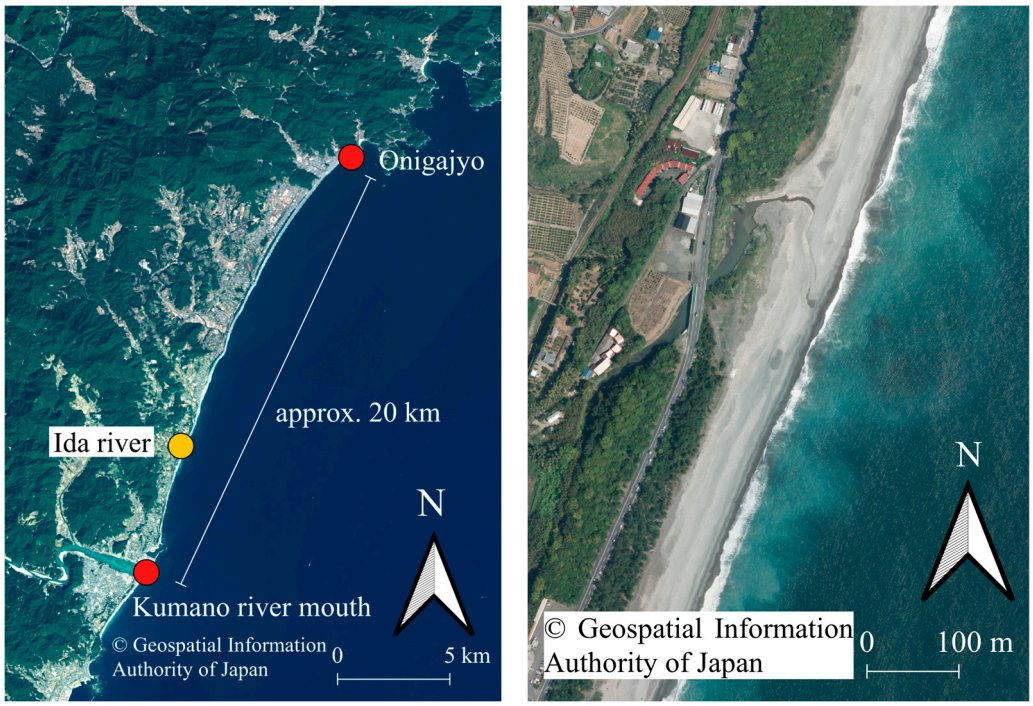
Citation: Torii, Y.; Kiku, M.; Mizutani, N.; Nakamura, T. Effectiveness of Staggered Pile Arrangements for Managing River Mouth Closures on Gravel Beaches. *J. Mar. Sci. Eng.* **2025**, *13*, 253. https://doi.org/10.3390/jmse13020253

Copyright: © 2025 by the authors. Licensee MDPI, Basel, Switzerland. This article is an open access article distributed under the terms and conditions of the Creative Commons Attribution (CC BY) license (https://creativecommons.org/licenses/by/4.0/).

1. Introduction

The Shichiri-Mihama coast, spanning 20 km from Kumano City—where the World Heritage Site, Onigajo, is located—to Kiho Town at the mouth of the Kumano River, is situated in the southern part of Mie Prefecture, Japan, as shown in Figure 1a. This region features the longest sand and gravel beach in Japan, into which several small- and medium-sized rivers flow. Key challenges in the Shihara River and at the Ida River estuary (Figure 1b), including the lack of rainwater runoff capacity and the river mouth closure due to dams built upstream of the Kumano River and coastal drift sand from the Kumano-nada Sea, are problems. Cases of estuary closure due to dam construction have also occurred overseas, such as on the delta coast of the Netherlands, and are being investigated [1]. Also, the Shihara River has experienced difficulties in maintaining flow despite river mouth management measures such as levee construction and riverbed excavation initiated in 1977. As the river mouth closure progresses, the risk of flooding along the inner banks increases during heavy rainfall, impacting the lives and properties of residents in the watershed area. Moreover, the formation of estuarine spits and bars is intensifying, a phenomenon that is not exclusive to Japan but is observed in rivers worldwide, adversely affecting

ecosystems [2,3]. From the viewpoint of nature conservation, it is important to prevent river mouth closure to overcome the poor river environment and to allow river water to circulate to the sea. Therefore, effective river mouth management strategies are crucial to optimize the functionality of river structures and maintain adequate flow capacity.



(**a**) (**b**)

Figure 1. Location of the study site: (**a**) position of the Shichiri-Mihama coast; (**b**) estuary of Ida River.

Although dike and embankment protection against river mouth closure is common for large rivers in Japan, such structural measures are rare for small- and medium-sized rivers. The narrower river mouths of these rivers necessitate specific interventions to ensure the maintenance of river channels and flow paths during floods. Research has been conducted to understand the dynamics of river mouth closures by assessing the risks and conditions associated with these closures [4], employing numerical models to simulate these processes [5], and using video cameras to monitor river mouth spits and shorelines [6], targeting regions globally where such closures are prevalent. Existing studies have been focused on the causes of estuary closures, but no measures have been proposed to control the formation of berms in estuary closures and to shift the location of the berm formation. This study addresses these issues by proposing a countermeasure using structure. Although hydraulic model experiments utilizing piles have been conducted worldwide [7], these primarily focus on understanding local scouring mechanisms around piles and examining coastal erosion countermeasures using piles [8], with few applications directed toward river mouth closures. Additionally, when piles are installed on sand, they tend to erode the sand surface owing to scouring around the pile. The depth of the scour varies depending on the pile configuration; the staggered piles, as opposed to a single row, typically form a horseshoe vortex that enhances erosion near the piles [9]. The related studies have mainly addressed sand surfaces and interactions between two or three piles [10,11], neglecting the effects of pile installations on gravel beaches or the impacts of configurations involving four or more piles. In this study, the countermeasure (staggered piles) using a group of four or more consecutive piles is proposed for a gravel beach. The proposed staggered piles solve the estuary closure phenomenon of the estuary connected to the gravel beach.

This study conducts hydraulic model experiments to examine effective pile installation as the countermeasure to estuary closures on gravel beaches. Piles are placed in a staggered and continuous manner to disrupt the gravel flow path and reduce gravel deposition in overland areas. The study compares the effect of the spacing between piles rows on gravel beach topography by varying in the offshore direction under diverse wave conditions, for example, how far offshore the placement of the piles advances the location of the berm formation, and how much they reduce the amount of sedimentation on land. To quantitatively evaluate these changes, the effective staggered piles installation is clarified from the three viewpoints of "reducing the maximum elevation of the berm", "advancing the location of the berm formation offshore", and "reducing the amount of sedimentation in the land area", in comparison with the topographical change without the continuous piles installation.

2. Summary of Hydraulic Model Experiments

2.1. Hydraulic Model of Gravel Beach

Hydraulic model experiments were conducted in a two-dimensional wave-generating channel, measuring 25 m in length, 0.70 m in width, and 1.0 m in height, at Gifu National College of Technology. Figure 2 shows a schematic of the experimental setup. A piston-type irregular-wave generator, controlled by signals from a control personal computer (PC), is positioned at one end of the channel. These signals are transmitted to a wave-making control panel, which then actuates the wave generator, generating waves within the channel. An impermeable slope, constructed from plywood and angle steel with a 1/7 gradient, is located 18.1 m from the wave generator. The experimental setup adhered to a 1/25 scale according to Froude's law of similarity. The slope was covered with a 15 cm layer of gravel, characterized by a median grain size (d_{50}) of 3.4 mm.

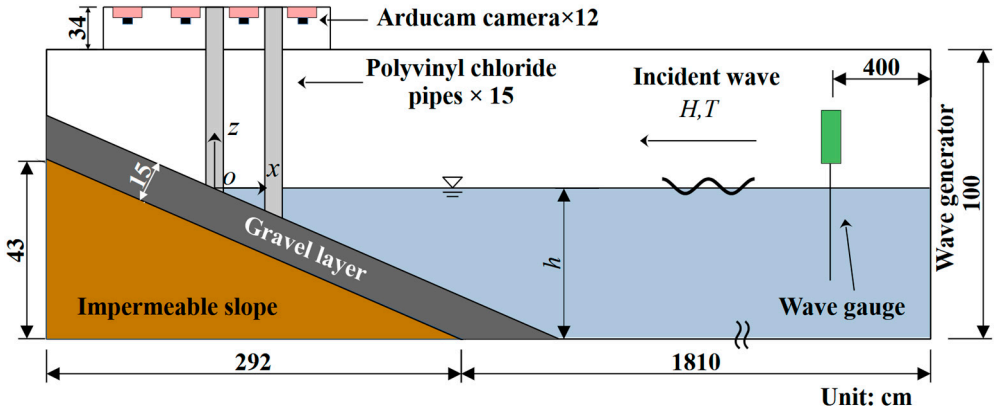


Figure 2. Schematic of experimental equipment.

2.2. Hydraulic Model of the Countermeasure for River Mouth Closure

Accelerated landward deposition of gravel significantly contributes to river mouth closures and reduces the river's capacity to transport water. Thus, relocating the berm formation from landward to offshore is crucial for maintaining the flow capacity of the estuary. In response, eight polyvinyl chloride (PVC) pipes, each with an outer diameter of 18 mm (equivalent to 450 mm in the field), were installed in a single row along the coastal direction at 10 cm intervals, starting from the initial shoreline position (x = 0.00 m), as shown in Figure 3. This arrangement aims to prevent river mouth closure without obstructing river flow. Additionally, a second row of staggered piles was placed on the offshore side to further control the movement of gravel and mitigate the impact of accelerated shore-side gravel deposition. The staggered configuration of the piles disrupts the path of upwelling

waves while ensuring the flow through the estuary remains unimpeded. In the schematic, red dashed lines indicate the beach side (row B), and blue dashed lines denote the seaside (row S). The experiment varied the distance between row B and row S from 10 cm to 20 cm, testing different configurations to determine their effectiveness in managing sediment transport and berm formation. The spacing of the staggered piles assumed that the wave flow path would be secured. The spacing was set in consideration of the distance between the piles, the number of piles that could be installed in relation to the width of the channel, and coordination with the measurement equipment installed above the channel.

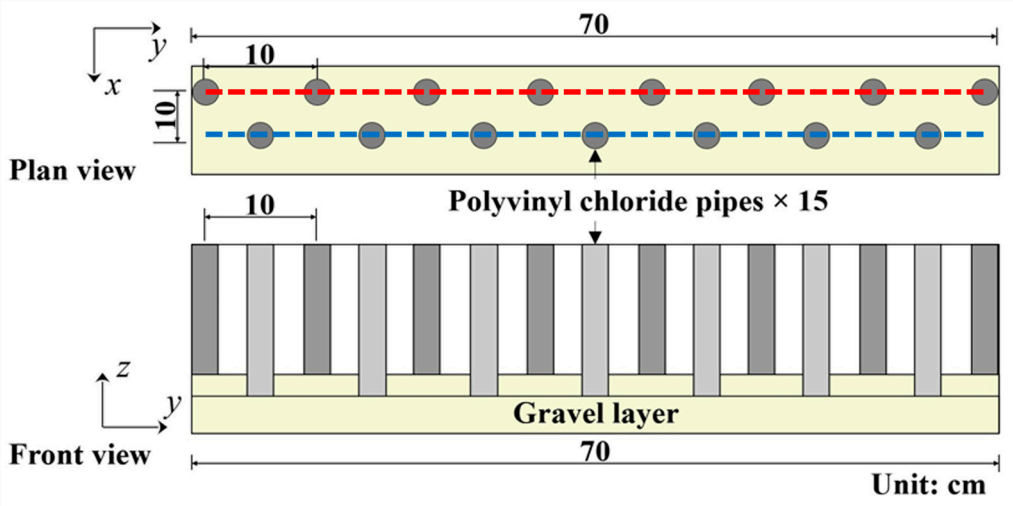


Figure 3. Schematic of the countermeasure.

2.3. Three-Dimensional (3D) Topographic Measurement Method

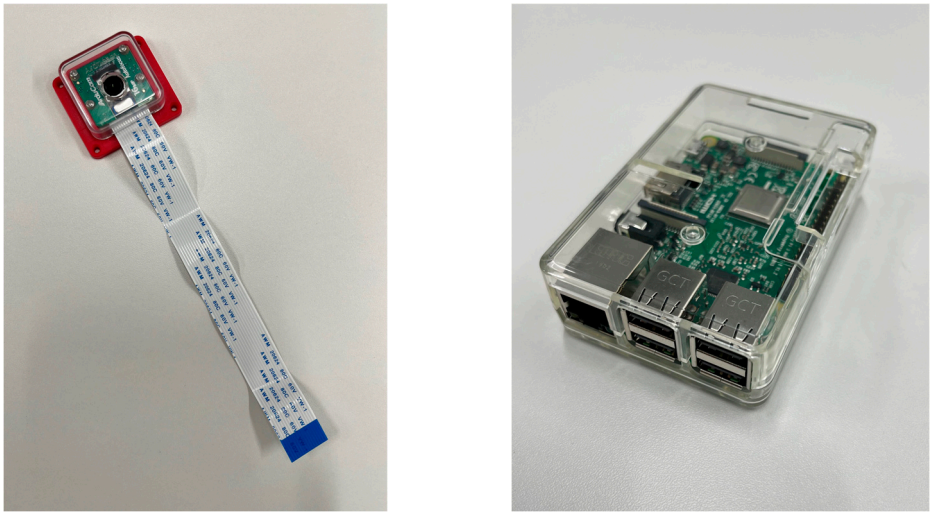
To assess the effects of the countermeasure on the dynamic topographic changes in gravel beaches, capturing the topography in three dimensions is essential. Therefore, the 3D topographic measurement method employed in this study utilizes an 16MP Autofocus Camera (hereafter referred to as "Arducam camera").

2.3.1. Using the Camera

Figure 4 shows the setup involving the Arducam camera paired with a Raspberry Pi 3B. Table 1 outlines the performance specifications of the Arducam camera. The connection interface between the Arducam camera and the Raspberry Pi 3B is the MIPI CSI-2 (Mobile Industry Processor Interface Camera Serial Interface-2). This interface facilitates the direct transfer of captured data to the memory of the Raspberry Pi 3B at a maximum rate of 1.2 Gbps, thereby enhancing the speed of image processing.

Table 1. Performance of camera.

Parameters	Arducam 16MP Autofocus Camera
Sensor	Sony IMX519
Optical size	1/2.53″
Sensor resolution	4656 × 3496 pixels
Still resolution	16 megapixels
Focus	Auto
Interface	MIPI CSI-2
Focal length	4.28 mm
Field of view	80°
Sensor dimension	7.103 mm diagonal
Height of installation	0.94 m
Ground coverage	1.56 m diagonal



(**a**) (**b**)

Figure 4. Structure of the 3D topographic measurement system: (**a**) Arducam 16MP Autofocus Camera; (**b**) Raspberry Pi 3B.

The system configuration involved connecting the Arducam camera to a Raspberry Pi 3B, which was programmed in Python to capture images at intervals of 0 and 30 s each minute. The Raspberry Pi 3B was linked to a Windows PC within an intranet environment, enabling remote access to all Raspberry Pi 3B units via VNC Viewer from the Windows PC. Notably, the Raspberry Pi 3B lacks a real-time clock, implying that it does not maintain time settings when powered off. While it is possible to automatically acquire and synchronize time from an NTP (Network Time Protocol) server that is accessible via the Internet, the hydraulic laboratory used for this study does not support an Internet-capable network environment. Therefore, we utilized a Windows PC as an NTP server to synchronize the time information across all 12 Raspberry Pi units, ensuring simultaneous image capture.

2.3.2. Camera and Marker Placement

In the creation of a 3D point cloud from aerial photographs taken by an unmanned aerial vehicle, the overlap rate between images is generally set at 80% or more. In this study, 12 Arducam cameras were placed in a row on the gravel beach slope, positioned at 9.1 cm intervals above the channel and at a height of 34 cm from the channel's top (Figure 5), ensuring a 90% overlap rate between images captured at the shoreline. Each camera was mounted on a wooden plate to stabilize its position and maintain consistent camera spacing.

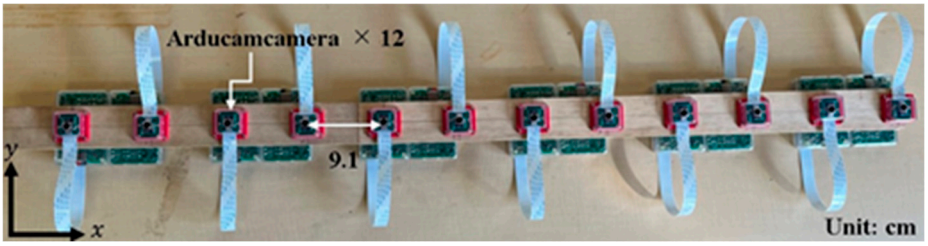


Figure 5. Camera position.

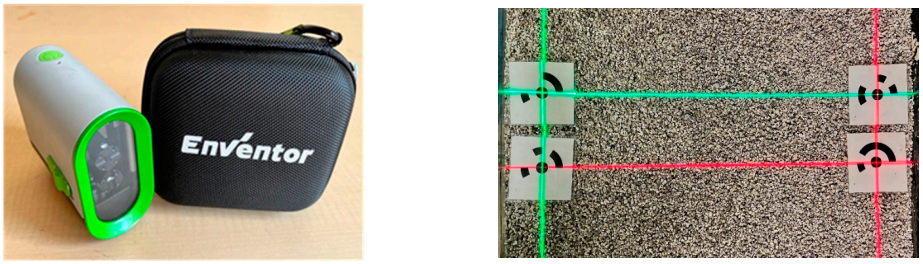
To generate a digital surface model (DSM) and an orthomosaic image of the gravel beach, the 3D-modeling software Agisoft Metashape ver.2.0.1 (Metashape) was used. Markers, serving as indicators of positional coordinates and distances, were crucial for this process. These markers were placed where they would not be obscured by run-up waves

(Figure 6). The intersection of the shoreline and the channel's center at a depth (h) of 40 cm was designated as the origin for the 3D model. The markers used were designed to be automatically recognized and numbered by Metashape.



Figure 6. Marker placement.

The experiment involved photographing the topography before, during, and after wave-making activities. During wave-making, 12 cameras installed above the channel captured images of the gravel beach at 30 s intervals, resulting in a total of 361 image sets. Before and after wave-making, the gravel beach in its drained condition was photographed by 12 cameras, with an additional four cameras repositioned offshore to capture a total of 16 images. Because markers could not be permanently installed on the offshore side, submerged during wave-making, two lasers were mounted to the top of the channel's sidewall (Figure 7a). The center of the marker was aligned with the four intersection points of the linear lasers (Figure 7b). The position of the laser on the gravel beach surface was fixed, and markers were positioned at known points whose X and Y coordinates had been previously measured by a total station. The Z-coordinate was measured by a laser rangefinder (Bosch GLM 50C) each time an image was captured, accommodating for topographic changes before and after wave creation.



(**a**) (**b**)

Figure 7. Laser and usage examples: (**a**) laser; (**b**) positioning of markers and laser.

2.3.3. D Model Construction and Accuracy of Model

As a result of the experiment, a 3D model was constructed from simultaneously captured images using Metashape. From this model, the numerical surface model DSM (Figure 8a) and the orthomosaic image (Figure 8b) were extracted. The "Accuracy" setting in the "Photo Alignment" process was set to "High" to enhance the precision of the model constructed from the captured images. The accuracy of the DSM has been examined [12]. In this study, the measurement accuracy of the DSM was confirmed by comparison with the actual values measured using the total station. The results show that the maximum root mean squared error (RMSE) of the measured values is less than 0.6 cm in XYZ coordinates under the condition of "High" for the analysis accuracy of the "Photo Alignment" process.

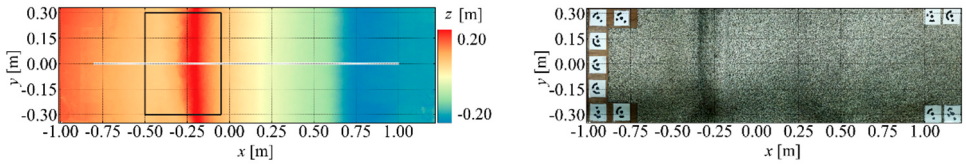


Figure 8. Topographic model extracted from 3D model: (**a**) DSM; (**b**) Orthomosaic image.

2.3.4. Results from the DSM

For this study, the cross-section in the center of the channel (x = 0.00 m), as indicated by the white line in Figure 8a, was extracted. The land area, defined as a segment measuring 0.45 m in length (-0.50 m $< x <$ -0.05 m) and 0.60 m in width (-0.30 m $< y <$ 0.30 m) and covering 0.27 m^2 as shown by the black box in Figure 8a, was analyzed for landform change. To minimize errors in calculating topographic change, the section from -0.05 m $< x <$ 0.00 m, which might be influenced by the countermeasure, was excluded from the calculation range.

The following content details the experimental results obtained during wave-making when regular waves with a height (H) of 8.0 cm and a period (T) of 2.0 s were applied for 3 h in a water depth (h) of 40 cm. Preliminary tests were conducted in advance to confirm whether the target waves were generated at 4.0 m from the wave generator. The cross-sectional topography at the channel center (y = 0.00 m) extracted from the DSM at each time point is shown in Figure 9. The dashed line in the figure represents the water surface. Owing to the limitations of the measurement method, it cannot accurately measure the topography under the water surface. So, the boundary between land and water was delineated using the orthomosaic image to except the influence of the water surface.

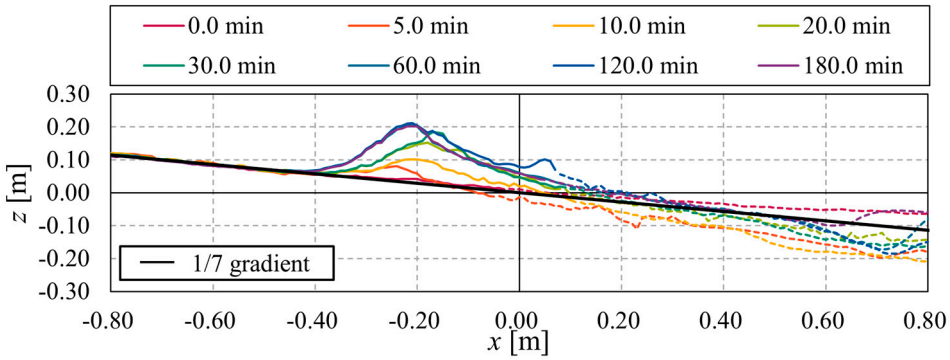


Figure 9. Topographic change in the cross-section in the center at the flume.

Figure 9 shows that at t = 0.0 min (initial topography), for $x > 0$, the dashed line indicates the water surface, which complicates the accurate reproduction of the topography. Meanwhile, for $x < 0$, the solid line shows the topography where the water surface does not affect measurements, the 1/7 gradient is accurately reproduced, indicating high reproducibility for landforms not in contact with the water. The figure shows that gravel accumulation began around $x = -0.20$ m from t = 5.0 min by t = 10.0 min, and this accumulation had increased to a height of z = 0.10 m above the initial topographic elevation of the shoreline, forming berm. The formation of the berm likely prevented the water surface's influence from extending further landward. This can be seen from the fact that the solid and dashed boundaries that mark the boundary between land and water are not located landward of the top of the berm.

Figure 10 shows the location of the maximum height at the center of the channel (y = 0.00 m) and its variation with height over time. The figure reveals that sedimentation

continued to progress until t = 60.0 min, stabilizing at approximately z = 0.20 m with x = −0.20 m at the peak.

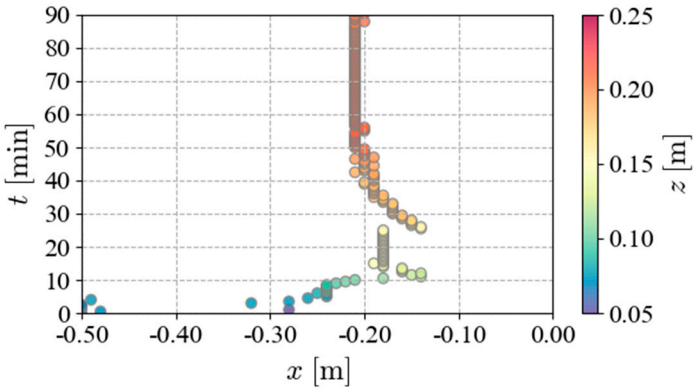


Figure 10. Changes in the position and height of maximum elevation at the center of the channel over time.

In this study, the effectiveness of the different piles' line spacing on the topography of a gravel beach was assessed using the 3D topography measurement method. This enables the visualization of cross-sectional topography at any given time, alongside the developmental process of the topography, comparing it with topography without a countermeasure.

2.4. Wave Conditions and Installation Conditions of the Countermeasure

In this experiment, the water depth was consistently maintained at h = 40 cm, while the wave period and height were varied to target a range of wave conditions, as detailed in Table 2. The wave steepness (H/L) was set to range from 0.020 to 0.031. The maximum wave height was set to H = 8.0 cm, given the limitations of the wave-generating system. The test waves were regular waves and were allowed to run for 3 h to ensure that the gravel beach topography reached equilibrium.

Table 2. Experimental conditions.

Case	Number of Experiments	Water Depth h [cm]	Wave				Countermeasure
			Height H [cm]	Period T [s]	Wave Length L [m]	Wave Steepness H/L	Interval of Installation Position d [m]
1-1	2	40	8.0	2.0	3.69	0.022	/
1-2	2	40	8.0	2.0	3.69	0.022	0.10
1-3	2	40	8.0	2.0	3.69	0.022	0.20
2-1	2	40	6.0	1.7	3.05	0.020	/
2-2	2	40	6.0	1.7	3.05	0.020	0.10
2-3	2	40	6.0	1.7	3.05	0.020	0.20
3-1	2	40	8.0	1.5	2.61	0.031	/
3-2	2	40	8.0	1.5	2.61	0.031	0.10
3-3	2	40	8.0	1.5	2.61	0.031	0.20
4-1	2	40	7.0	1.7	3.05	0.023	/
4-2	2	40	7.0	1.7	3.05	0.023	0.10
4-3	2	40	7.0	1.7	3.05	0.023	0.20
5-1	2	40	8.0	1.7	3.05	0.026	/
5-2	2	40	8.0	1.7	3.05	0.026	0.10
5-3	2	40	8.0	1.7	3.05	0.026	0.20

The experiment was designed to assess the impact of the countermeasure and the spacing between pile rows in the offshore direction on topographical changes. Three setups were tested: one without the countermeasure, one with a 10 cm distance between staggered rows B and S, and one with a 20 cm distance between staggered rows B and S, increasing the distance by 10 cm in the offshore direction. Each setup was replicated twice to verify reproducibility. This study specifically focused on the berms, investigating the effect of the countermeasure on the landform change. To study potentially hazardous scenarios, the configuration where the berm's maximum elevation was shoreward was selected.

3. Effects of Different Wave Conditions on Topographic Changes in Gravel Beaches

3.1. Comparison of Final Topography and Shoreline Location Without Countermeasure

The DSM of the final topography without the countermeasure is shown in Figure 11. In the figure, the berm at $z = 0.00$ m is marked with a black line. This figure reveals that, without the countermeasure, the shoreline position after the topography has equilibrated varies with the wave conditions. In all cases, the waves propagated further offshore than before wave formation. The location of berm formation, which occurs near $x = -0.25$ m, does not depend on the magnitude of H/L. As shown in Cases 1 and 2 (Figure 11a,b), a smaller H/L ratio results in a higher berm elevation and a tendency for the shoreline position to advance further offshore. These observations confirm that the shoreline position, berm elevation, and berm location are influenced by the H/L ratio.

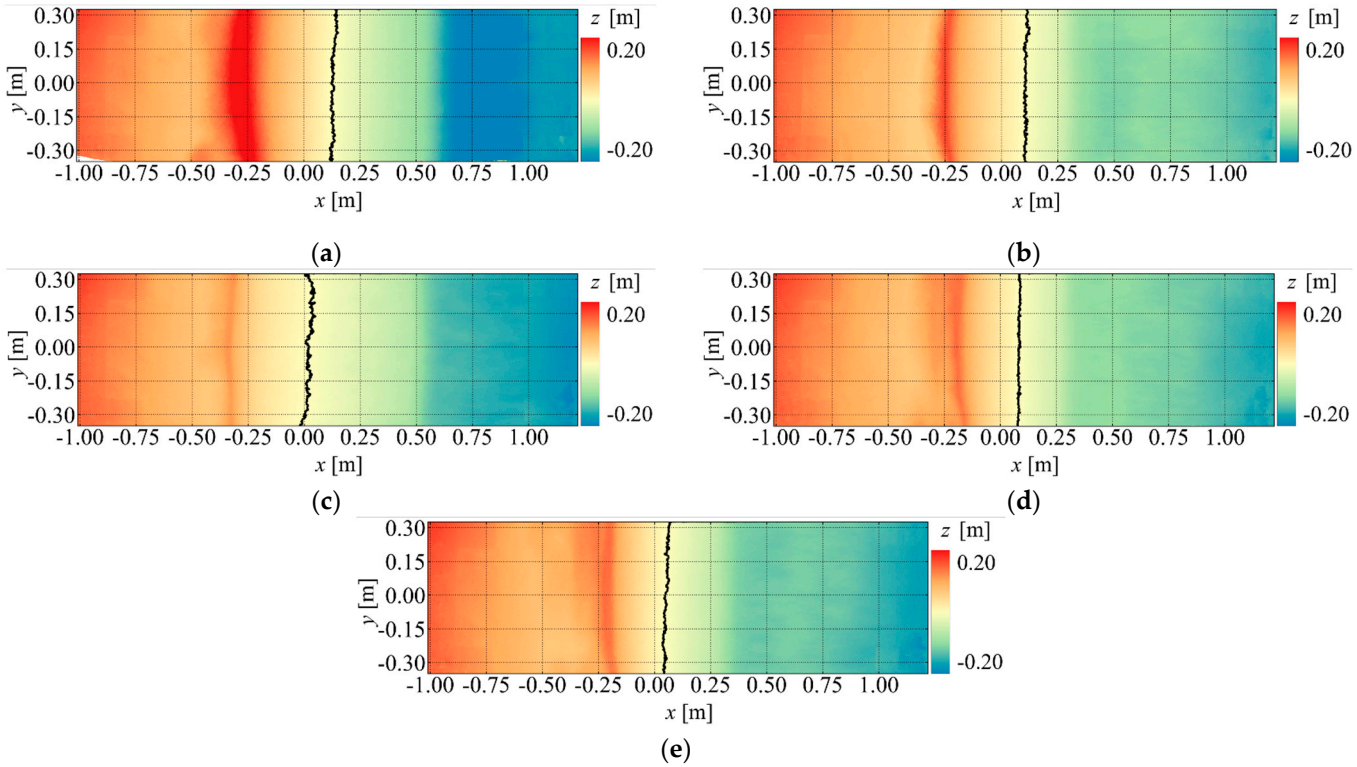


Figure 11. Final topography and position of shoreline on DSM: (**a**) Case 1-1; (**b**) Case 2-1; (**c**) Case 3-1; (**d**) Case 4-1; (**e**) Case 5-1.

3.2. Change over Time in Gravel Beach Topography

3.2.1. Change in Cross-Sectional Topography over Time Without Countermeasure

The cross-sectional topography of the channel center ($y = 0.00$ m) was extracted from the DSM at eight time points: $t = 0.0$, 5.0, 10.0, 20.0, 30.0, 60.0, 120.0, and 180.0 min from the

start of wave-making, as shown in Figure 12. The dashed line indicates the water surface, and the solid line indicates the topography. Owing to limitations in measuring beneath the water surface, the boundary between land and water was identified using the orthomosaic image to delineate the water surface. The times when there were missing measurements due to upwelling during wave-making are not shown in the figure because the model could not be generated.

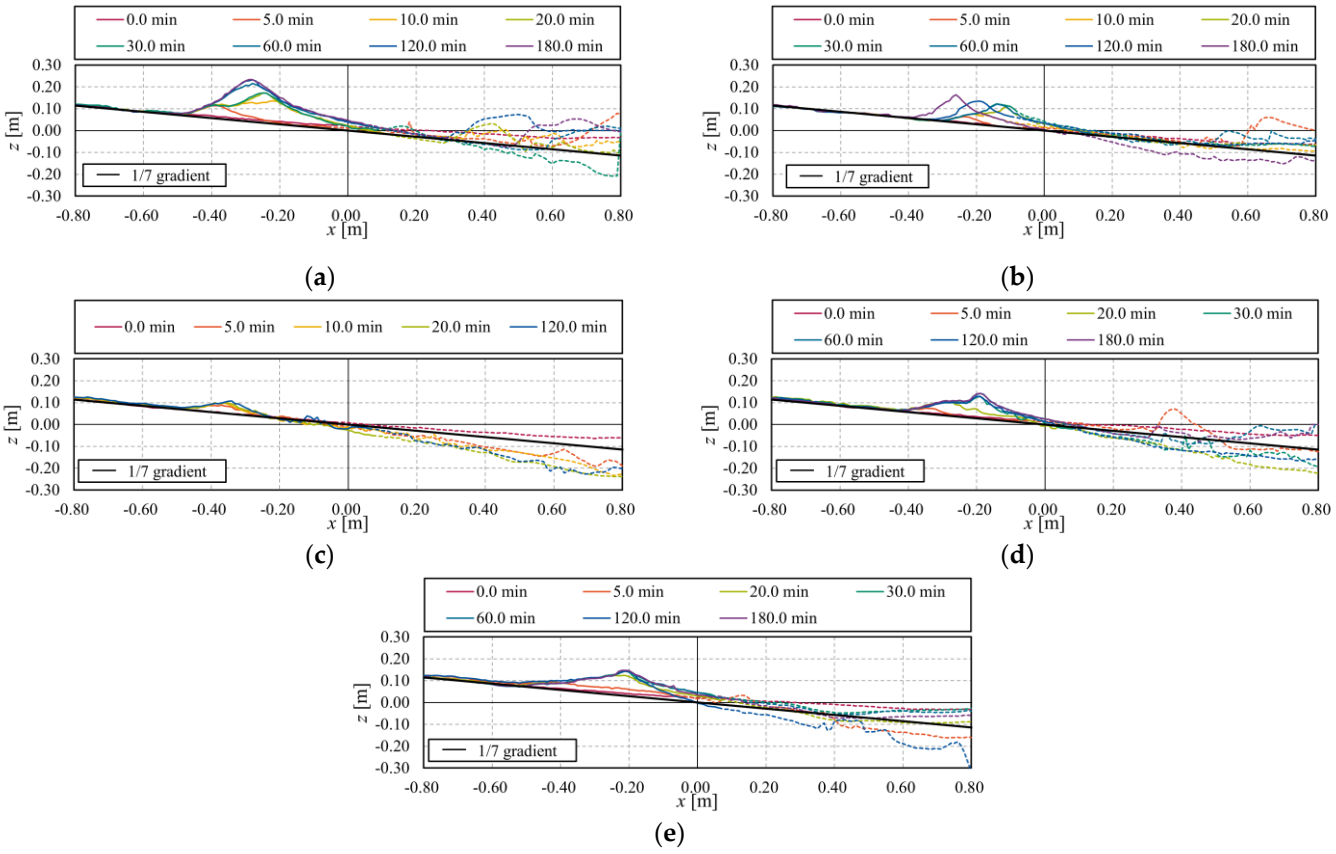


Figure 12. Change in topography of cross-section over time without countermeasure: (**a**) Case 1-1; (**b**) Case 2-1; (**c**) Case 3-1; (**d**) Case 4-1; (**e**) Case 5-1.

As shown in Figure 12a,b,d, the topography under conditions of a small H/L continues to change beyond t = 20.0 min, indicating that a longer time is required to reach equilibrium compared to scenarios with a larger H/L. The characteristic without the staggered piles is that, under most wave conditions except those in Case 2-1, the landward-most topography of the berm remains unchanged from the onset of wave-making to the end, with gravel accumulating in front of the berm. This pattern confirms that the process of the landform change varies with the wave conditions.

3.2.2. Change over Time in Maximum Elevation Position over Land Without Countermeasure

Figure 13 shows the time-series variation in the maximum elevation from the shoreline to the shore (-0.50 m $< x <$ 0.00 m). The highest elevation at $x = -0.50$ m is observed immediately after the start of wave generation owing to the constant slope. The figure indicates that the position of maximum elevation shifts over time as gravel accumulates from run-up waves. In all cases except Case 3-1, the location of the maximum elevation advances from the shore side to the offshore side by t = 20.0 min. The process of landform change varies with the magnitude of H/L: in Cases 1-1 and 2-1, the position of maximum elevation retreats toward the shore side, while in Cases 4-1 and 5-1, it remains in a fixed

position. In Case 3-1, there is no change in the position of maximum elevation from the beginning to the end of wave-making.

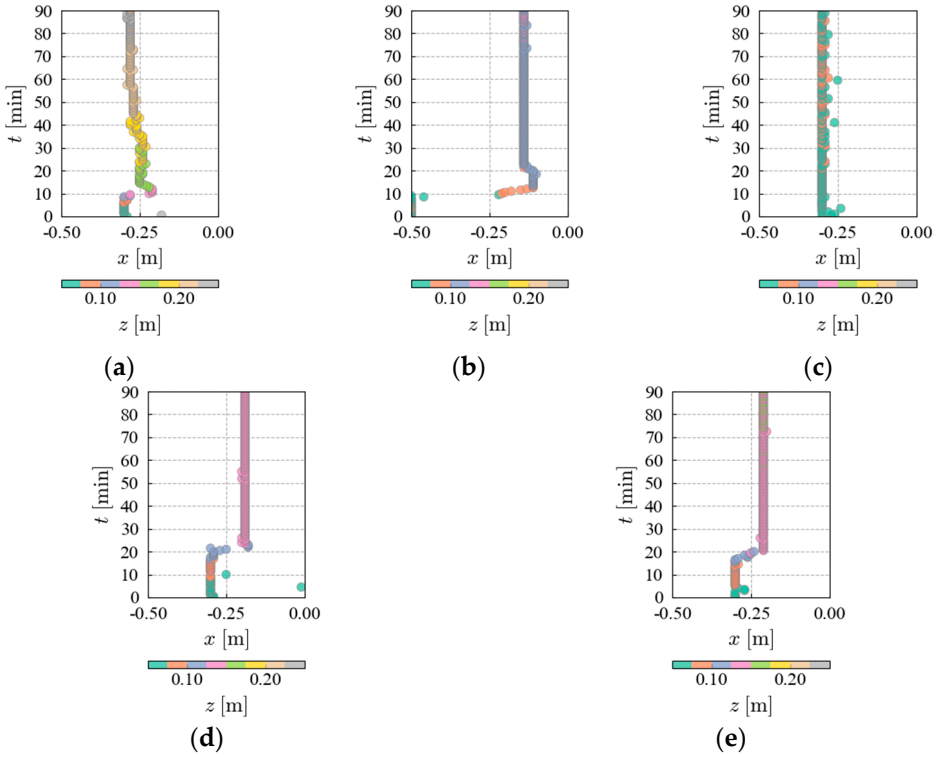


Figure 13. Change in maximum elevation (-0.50 m $< x <$ 0.00 m): (**a**) Case 1-1; (**b**) Case 2-1; (**c**) Case 3-1; (**d**) Case 4-1; (**e**) Case 5-1.

3.3. Amount of Topographic Change Without the Countermeasure

The amount of sedimentation in each case, calculated from the positive difference in elevation derived from DSM comparisons between the initial and final topographies, is presented in Table 3. Case 1-1 exhibits a significantly greater landform change compared to other cases, with sedimentation up to 5.9 times higher, confirming that the extent of sedimentation varies with the magnitude of H/L.

Table 3. Amount of landform change without countermeasure.

Case	Amount of Sediment [cm^3]
1-1	23,796
2-1	9999
3-1	4032
4-1	11,250
5-1	12,194

4. Topographic Change with Staggered Countermeasure (d = 10 cm)

4.1. Comparison of Final Topography and Shoreline Location (d = 10 cm)

The DSM of the final topography, when the distance between rows B and S is 10 cm, is shown in Figure 14. Similarly to the no-countermeasure scenario, the shoreline (z = 0.00) m in the final topography is indicated by a black line. The impact of the staggered piles on the landform changes was assessed by comparing them to the case without the countermeasure.

In all cases, the shoreline position in the final topography advanced offshore from the initial shoreline position. In contrast to the no-countermeasure case, there was no

consistent tendency for the shoreline position to advance further offshore. The staggered piles influenced the advancement of the shoreline position, although the variation in shoreline position due to different wave conditions was minimal. However, the extent of movement was confirmed to be less than 0.10 cm.

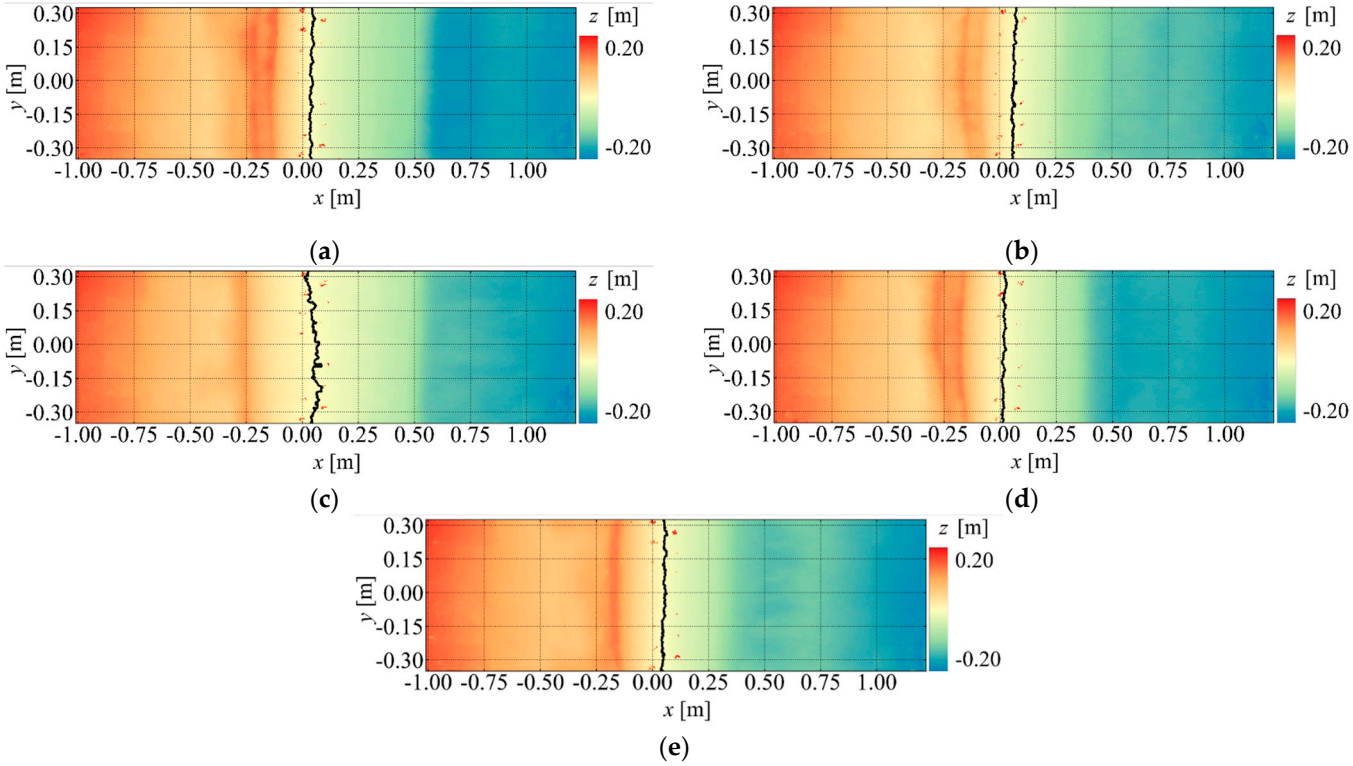


Figure 14. Final topography and position of shoreline on DSM: (**a**) Case 1-2; (**b**) Case 2-2; (**c**) Case 3-2; (**d**) Case 4-2; (**e**) Case 5-2.

As shown in Figure 14a,b,d, a smaller H/L ratio results in a wider berm in the offshore direction. In these cases, the berm's shape differed from that in the case without the countermeasure, exhibiting two peaks. This suggests that the countermeasure may have influenced the berm formation process. Observations during the experiment indicated that the amount of gravel rolled up by breaking waves increased as H/L decreased. Under wave conditions with a small H/L, the staggered piles complicated the flow path and weakened the force of the upwelling waves, which had a remarkable inhibiting effect on the gravel run-up.

The staggered arrangement proved effective in moving the location of the berm formation offshore or lowering the elevation of the berm. Additionally, the impact of wave conditions on the berm shape, in the absence of the staggered piles, was confirmed.

4.2. Effects of Countermeasure on the Process of Topographic Change (d = 10 cm)

4.2.1. Change in Cross-Sectional Topography over Time (d = 10 cm)

Figure 15 shows the cross-sectional topography at the center of the channel (y = 0.00 m) extracted from the DSM at each time point. Similarly to the scenario without the countermeasure, the dashed line represents the water surface. Figure 15a,b,d reveal that in cases of a relatively small H/L, two distinct mounds form in the land area, which is a divergence from the case without the countermeasure. These characteristic landforms begin to appear after t = 20.0 min from the start of wave-making and stabilize after t = 30.0 min. The smaller the H/L value, the more gravel is propelled and run up to the landward side. However, the staggered piles mitigate the wave force, preventing the gravel from running

up excessively and thus causing gravel to accumulate at the front of the berm and near the initial shoreline position. However, as shown in Figure 15c,e, in cases of a relatively large H/L, the staggered piles that altered the berm shape were less effective.

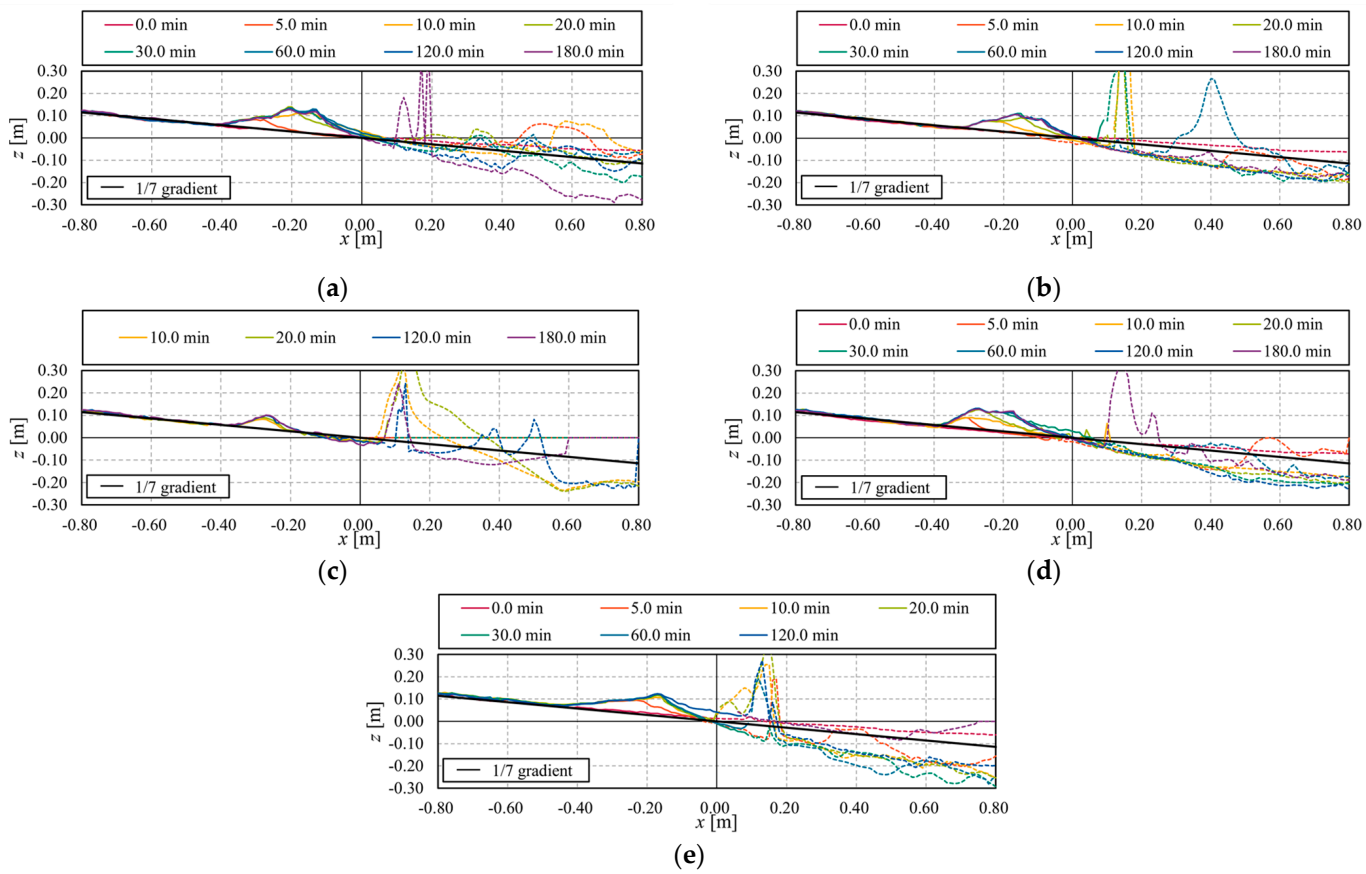


Figure 15. Change in topography of cross-section over time with countermeasure (d = 10 cm): (**a**) Case 1-1; (**b**) Case 2-1; (**c**) Case 3-1; (**d**) Case 4-1; (**e**) Case 5-1.

In comparison to the case without the countermeasure, no instance shows continuous landform change from immediately after the start of wave-making to the end, and the berm formation tends to stabilize by t = 30.0 min at the latest. The staggered piles may have established the location of berm formation earlier and further offshore, thereby inhibiting the berm's development over time.

Staggered pile arrangements in the case of a sandy bottom have been studied for the scour phenomenon. In the case of sand, the scour depth of staggered piles is larger than that of a single pile. In this study, it is necessary to examine whether the same landform change occurs on a sandy beach as on a gravel beach, not considering longshore flow, and that the bottom material is gravel [13].

4.2.2. Change over Time in Maximum Elevation Position over Land (d = 10 cm)

Figure 16 shows the time-series variation in the maximum elevation on the shore side of the berm (-0.50 m $< x <$ 0.00 m). The elevation at $x = -0.50$ m is the highest immediately following the start of wave generation, owing to the constant slope.

Figure 16a,b,d reveal that in cases of a relatively small H/L, determining the maximum elevation position of the berm takes time, and the maximum elevation also increases over time. However, in all cases, the time required to establish the maximum elevation was the same or shorter than in the case without the countermeasure. The staggered piles tend to fix the location of the berm formation at an early stage and promote topographic stabilization.

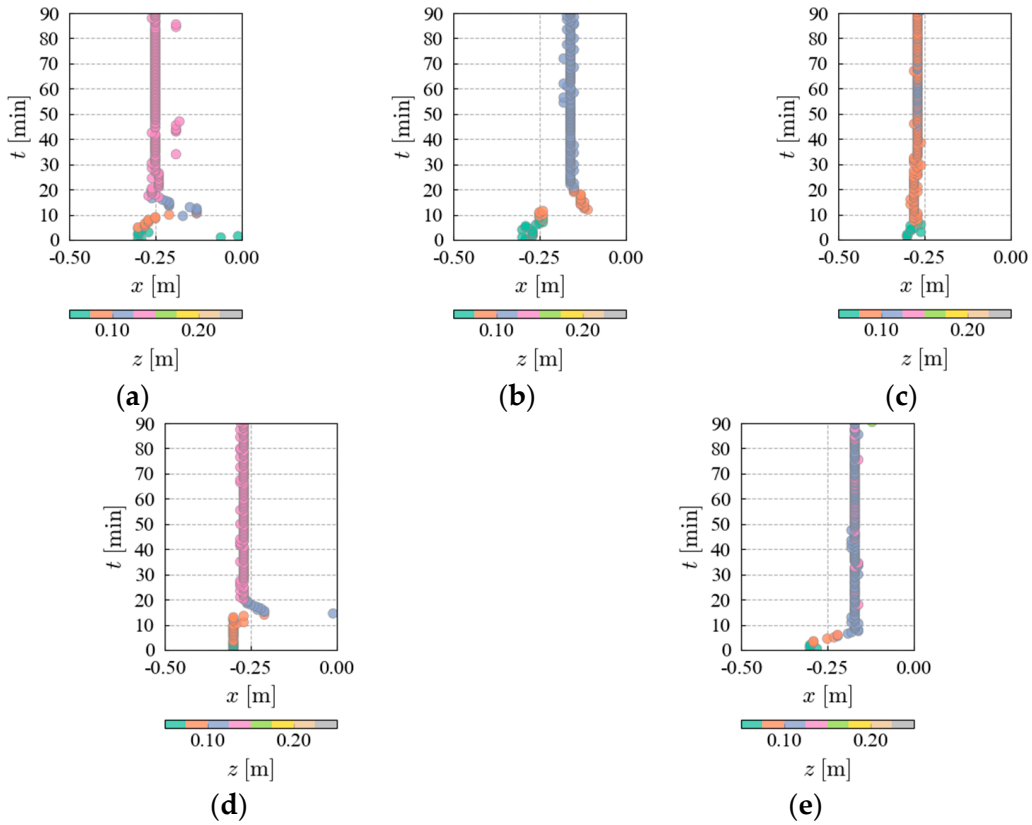


Figure 16. Change in maximum elevation (-0.50 m $< x <$ 0.00 m): (**a**) Case 1-2; (**b**) Case 2-2; (**c**) Case 3-2; (**d**) Case 4-2; (**e**) Case 5-2.

Compared to the case without the countermeasure, the location of the maximum elevation at the time of topographic stabilization is not necessarily more offshore owing to the staggered piles. Additionally, as shown in Figure 16c, the maximum elevation of the berm tends to increase with countermeasure, suggesting that certain wave conditions may enhance the formation of the berm.

4.3. Amount of Topographic Change with Countermeasure

The amount of sedimentation in each case, calculated using the positive difference in elevation derived from DSM comparisons between the initial and final topography, is shown in Table 4. Negative values indicate an increase in sedimentation relative to the case without the countermeasure. For instance, Case 1-2 exhibited the largest amount of sedimentation, yet this amount was reduced by approximately 57% compared to the case without the countermeasure. Meanwhile, in Case 3-2, the amount of sedimentation increased following the installation of the staggered piles. In this case, where the amount of debris transported was small, the installation of the countermeasures reduced the flow volume and increased the velocity of the upwelling waves passing through the pile, resulting in the transport of a large amount of debris to the land area. Therefore, while the installation of the staggered piles generally reduced the amount of gravel deposited on the shore side, under conditions with large H/L ratios, the accumulation of gravel on the shore side was intensified.

Table 4. Amount of landform change with countermeasure (d = 10 cm).

Case	Amount of Sediment [cm^3]	Amount of Decrease (Comparison Without Countermeasure) [cm^3]
1-2	13,465	10,331
2-2	7804	2195
3-2	4912	−880
4-2	11,429	−179
5-2	9210	2984

5. Topographic Change with Different Plie Row Intervals of Continuous Piles (d = 20 cm)

In the previous section, the effectiveness of the countermeasure was assessed under various wave conditions. Although the staggered piles advanced the location of the berm, they did not consistently reduce the maximum elevation of the terrain. The amount of sedimentation on land varied with wave conditions, indicating that large H/L ratios may promote sedimentation, particularly under large wave conditions. The denser the arrangement of the staggered piles that impede the gravel's upstream path, the greater the risk of inhibiting river flow. Owing to the experimental setup, the distance between each row of pile rows in the offshore direction along the longshore could not be altered. Furthermore, increasing the distance of the placement in the longshore direction could diminish the effectiveness of the staggered piles and widen the gravel's upstream path, potentially promoting estuary closure. This study compares and examines the effects of the staggered of B and S rows on beach topography when the distance between the rows is increased in the offshore direction.

5.1. Comparison of Final Topography and Shoreline Location (d = 20 cm)

Figure 17 shows the DSM of the final topography with staggered piles when the distance between rows B and S is increased to 20 cm in the offshore direction. The shoreline at z = 0.00 m in the final topography is marked with a black line, as in the case without the countermeasure.

In all cases, the shoreline advanced further offshore than before the adjustment of the staggered piles' distance. However, there was no significant tendency for the shoreline position to advance further offshore compared to the case without the countermeasure. Widening the distance between the staggered piles in the offshore direction confirmed the effect of moving the shoreline further offshore. The staggered arrangement, with row S advanced offshore, appears to have diminished the impact of the gravel carried by the run-up waves, thereby expanding the area where gravel accumulated above z = 0.00 m offshore, resulting in the shoreline advancing further offshore.

Figure 17 also indicates that in all cases, the berm elevation was lower compared to the case without the countermeasure. However, the effect of reducing the berm elevation by altering the distance between the placement of continuous piles was minimal. Notably, in Case 1-3, as shown in Figure 17a, the berm elevation exceeded 0.20 m, similar to the case without the countermeasure. This is because the wider distance between the continuous piles reduced the complexity of the flow path characteristic of the staggered arrangement, thereby allowing gravel to pass more freely. The location of the berm advanced offshore compared to the case without the countermeasure, irrespective of the magnitude of H/L. Additionally, under conditions with a small H/L, the berm widened in the offshore direction, as with d = 10 cm, resulting in a distinctive shape with two peaks. The staggered piles' installation reduced the force of the waves impacting them, and the gravel continued to accumulate at the front of the berm, causing the berm to widen in the offshore direction.

Thus, the distance between the rows of piles influences both the height of the berm and the position of berm formation.

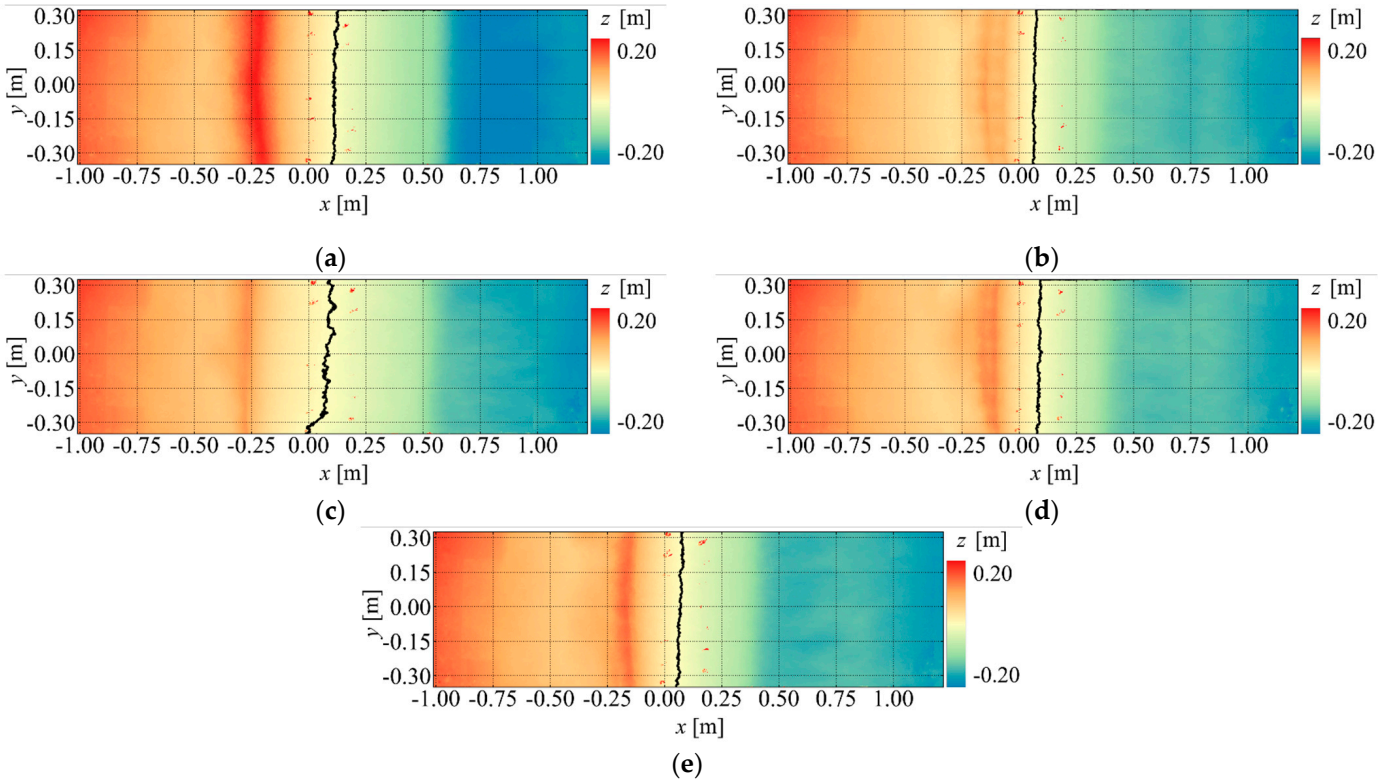


Figure 17. Final topography and position of shoreline on DSM: (**a**) Case 1-3; (**b**) Case 2-3; (**c**) Case 3-3; (**d**) Case 4-3; (**e**) Case 5-3.

5.2. Effects of the Countermeasure on the Process of Topographic Change (d = 20 cm)

5.2.1. Change in Cross-Sectional Topography over Time

Figure 18 shows the cross-sectional topography at the channel center (y = 0.00 m) extracted from the DSM at each time point. The dashed line indicates the water surface, and the solid line indicates the topography. As in the case without the countermeasure, the dashed line represents the water surface. In some cases, with a relatively small H/L, as shown in Figure 18b,d, two peaks form, differing from the case without the countermeasure. However, the occurrence of this characteristic topography decreased with the widening distance between the continuous piles. A topographic change that forms two mountains on land will reduce the maximum elevation of the berm. To make characteristic topographic changes, the pile row spacing should be shortened to ensure the complexity of the staggered piles.

Compared to before the widening of the pile row distance, there were fewer cases where the topography stabilized within t = 30.0 min from the start of wave-making, irrespective of the magnitude of H/L. Particularly, in Case 1-3, shown in Figure 18a, after the berm formation location stabilized, the elevation gradually increased and moved shoreward, showing a topographic change similar to that without the countermeasure. Increasing the spacing between staggered piles appears to delay the time required for the topography to stabilize.

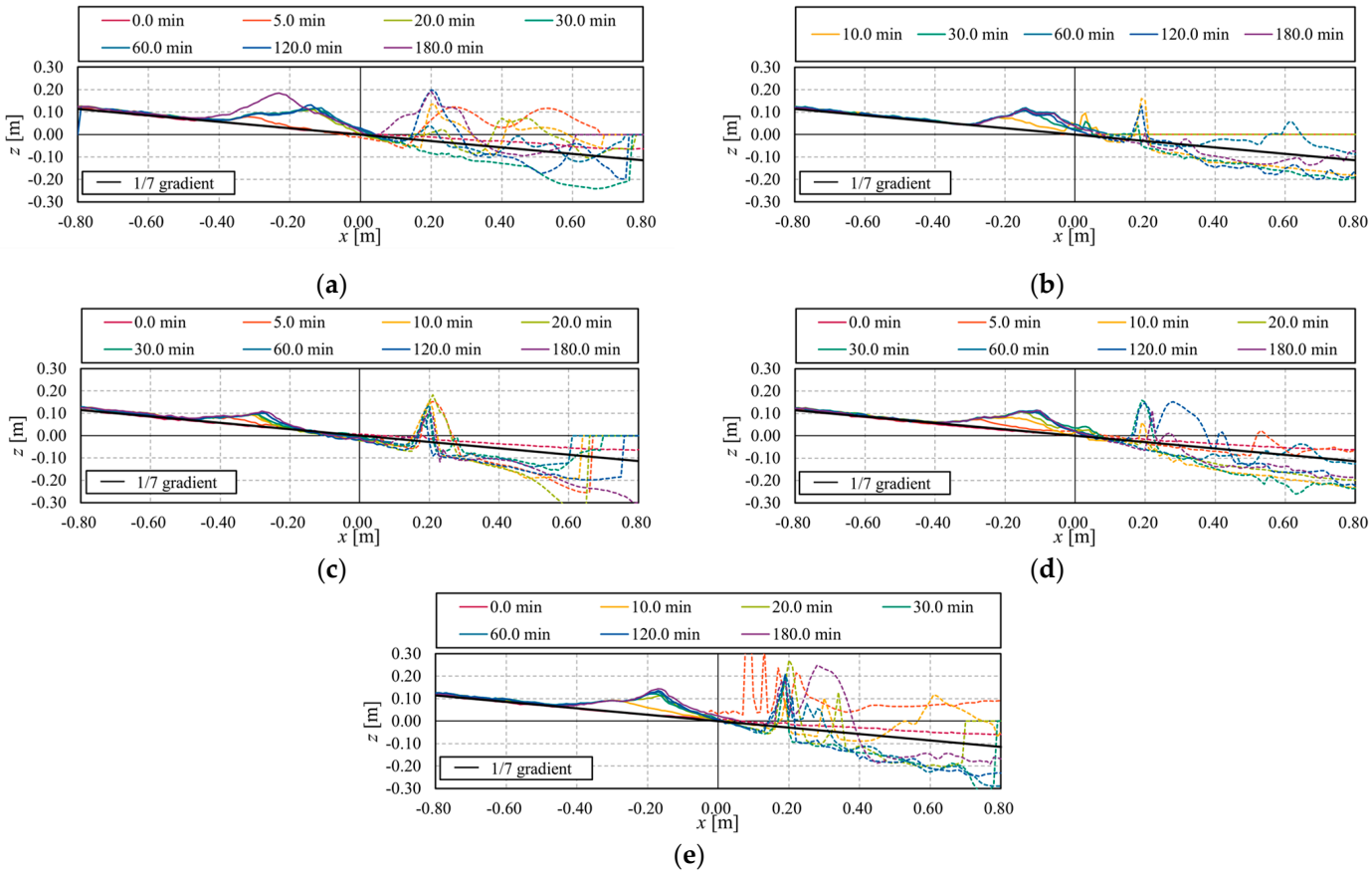


Figure 18. Change in topography of cross-section over time (d = 20 cm): (**a**) Case 1-3; (**b**) Case 2-3; (**c**) Case 3-3; (**d**) Case 4-3; (**e**) Case 5-3.

5.2.2. Change over Time in Maximum Elevation Position over Land (d = 20 cm)

Figure 19 shows the time-series variation in the maximum elevation on the shore side of the berm (-0.50 m < x < 0.00 m). The elevation at $x = -0.50$ m is the highest immediately following the start of wave generation, owing to the constant slope.

In all cases, no instances were observed where the maximum elevation or its position was determined by t = 20.0 min after the start of wave-making. Given that determining the maximum elevation position in each case takes time, the effect of increasing the distance between pile rows was confirmed to delay the time required for the topography to stabilize. In cases of a relatively small H/L, as shown in Figure 19a,b,d, the effect of advancing the maximum elevation position to $x = -0.15$ m by t = 10.0 min after the start of wave-making was evident. The offshore advancement of the S row of piles in a series of piles may have reduced wave momentum further offshore and shortened the gravel transport distance, resulting in an earlier advancement of the maximum elevation position of the berm than before the widening of the pile row distance.

5.3. Amount of Topographic Change When the Distance Between Continuous Piles Is Widened

The amount of sedimentation in each case, calculated using the positive difference in elevation from the DSM comparison between the initial and final topography, is presented in Table 5. Negative values indicate an increase in sedimentation compared to the case without the countermeasure. Increasing the distance between pile rows reduced the amount of gravel accumulated on the shore side in most cases, except for Case 3-3. In Case 3-3, where the landform change was minimal, the amount of sedimentation on the bank side increased, similar to before the widening of the pile row distance. The staggered piles' installation reduced the flow volume and increased the velocity of the waves running up

between the piles, which likely facilitated the transport of gravel to the shore compared to the case without the countermeasure. The increased distance between pile rows may have simplified the gravel transport paths impacted by the countermeasure, thus diminishing their effect on reducing the force of the upstream gravel.

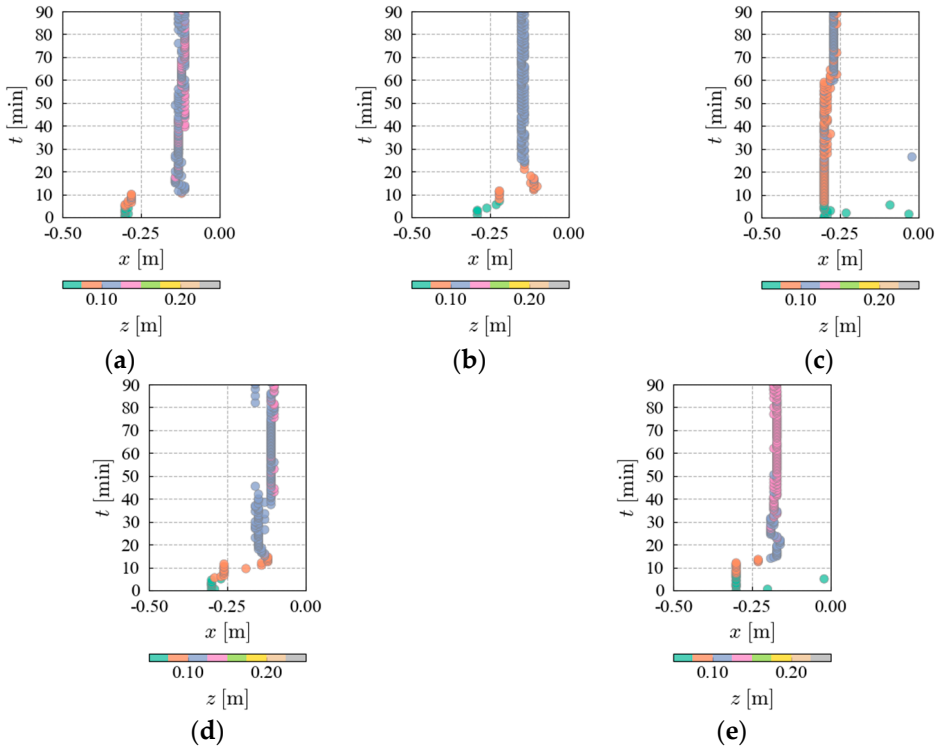


Figure 19. Change in maximum elevation (-0.50 m $< x <$ 0.00 m): (**a**) Case 1-3; (**b**) Case 2-3; (**c**) Case 3-3; (**d**) Case 4-3; (**e**) Case 5-3.

Table 5. Amount of landform change with countermeasure (d = 20 cm).

Case	Amount of Sediment [cm^3]	Amount of Decrease (Comparison Without Countermeasure) [cm^3]
1-3	19,045	4751
2-3	7086	2913
3-3	6421	−2389
4-3	9420	1830
5-3	11,786	408

6. Effectiveness of the Countermeasure Installation Conditions on Gravel Beaches

The influence of the countermeasure on the landform change varies with wave conditions and the spacing of the pile rows, affecting the formation process and final topography of the berm. However, results from hydraulic model experiments are scaled down to fit the experiment's scope, which aids in understanding the characteristics of the landform change under each wave condition but complicates quantitative evaluations that consider local applicability. To quantitatively demonstrate the effectiveness of the countermeasure, three effects were evaluated based on wave steepness (H/L) and the gravel beach profile when no countermeasure were installed: reducing the maximum elevation of the berm, moving the location of the berm formation offshore, and reducing sedimentation in the overland area.

6.1. Effect of Countermeasure Construction on Maximum Elevation of Berm

From the DSM of the final topography, the maximum elevation (z_{max}) of the central cross-section of the channel was extracted and made dimensionless by wave heights for each wave condition. Figure 20 compares the relationship between H/L and the dimensionless maximum elevation of the berm with and without the countermeasure and by the distance of placement.

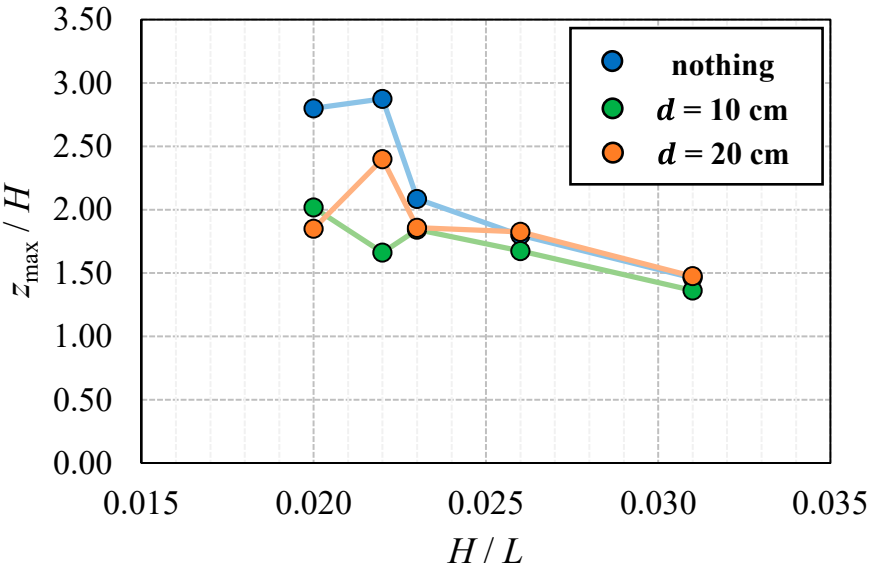


Figure 20. Relationship between wave steepness and dimensionless maximum elevation.

Figure 20 shows that when the distance between rows B and S of the piles is 10 cm, the staggered piles effectively lower the non-dimensional maximum elevation (z_{max}/H) of the berm under all wave conditions. Particularly under conditions where H/L is less than 0.023, the impact of lowering the final topography z_{max}/H by the countermeasure is notable. This effect is attributed to the staggered piles weakening the force of waves running up the gravel beach, which allowed gravel to continue accumulating at the front of the berm, widening the deposition area in the offshore direction. Meanwhile, under wave conditions where H/L is greater than 0.026, the difference between scenarios with and without the countermeasure is minimum. The larger H/L is, the smaller the wave-breaking zone similarity parameter obtained by Equation (1) becomes, which means that less gravel is swept up by the breaking waves and the staggered piles are not effective. Where β is the slope gradient and H/L is the wave steepness,

$$\xi = \tan\beta/(H/L)^{1/2} \quad (1)$$

For a 20 cm distance between rows B and S of a series of piles, no difference in z_{max}/H is observed without the countermeasure under wave conditions with an H/L greater than 0.026; however, under conditions with an H/L less than 0.023, the effect of lowering z_{max}/H on the final topography is confirmed. However, there are some wave conditions, such as when H/L = 0.020, where a wider spacing of the staggered piles would be more effective in reducing the maximum elevation.

The findings indicate that the staggered arrangement of the staggered piles reduces the maximum elevation of the berm for waves with a small H/L, regardless of the pile row distance. The effective placement condition in this study is to shorten the pile row spacing to 10 cm rather than 20 cm. This maintains the complexity of the staggered arrangement and is effective in reducing the maximum elevation of the berm for various waves.

6.2. Effect of Countermeasure Construction on Maximum Elevation Position of Berm

From the DSM of the final topography, the maximum elevation position (x) of the central cross-section of the channel was extracted and made dimensionless by wavelength for each wave condition. Figure 21 compares the relationship between H/L and the dimensionless maximum elevation position of the berm (x/H) with and without the countermeasure and by the distance of the pile-row arrangement.

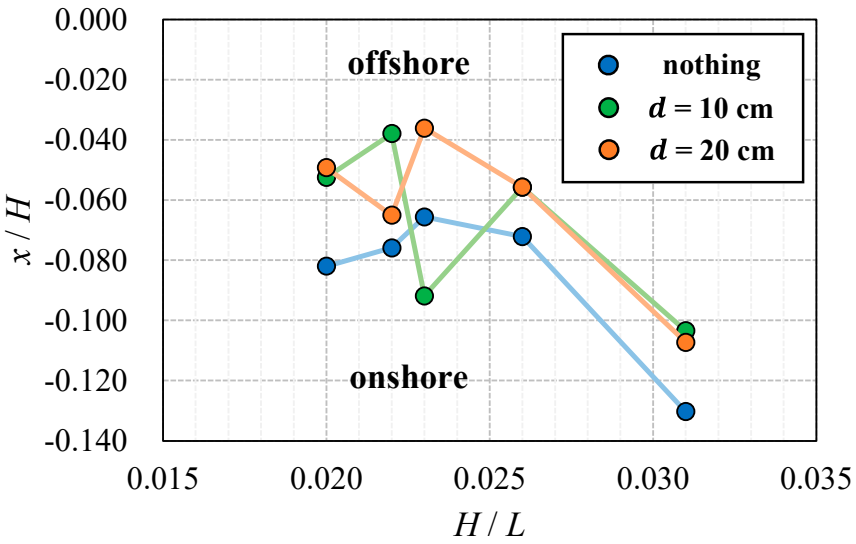


Figure 21. Relationship between wave steepness and dimensionless maximum elevation position.

The figure indicates that staggered piles effectively advance to the maximum elevation of the berm under a variety of wave conditions, regardless of the arrangement interval of the continuous piles. However, when the distance between rows B and S of the continuous piles is 10 cm, and H/L is 0.023, x/H is positioned more shoreward than in scenarios without the countermeasure. The cross-sectional topography in the center of the channel, as shown in Figure 22, indicates the formation of two mounds on land, a trend that is also observed in several other cases with continuous piles installed. Although x/H is larger than in the case without the countermeasure, the installation of the staggered piles is considered effective in reducing the maximum elevation of the berm over time and in accumulating gravel in front of the berm.

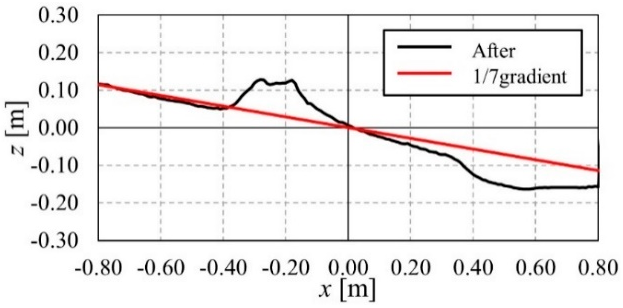


Figure 22. Cross-sectional topography in Case 4 (H/L = 0.023, d = 10 cm).

These results reveal that the staggered piles move the maximum elevation of the berm forward offshore under all wave conditions, regardless of the distance between the continuous piles.

6.3. Effect of the Countermeasure on the Amount of Sedimentation in the Land Area

The amount of topographic change was calculated from the DSM of the initial and final topography by measuring the differences in the area shown in the black box in Figure 8a. Among these landform changes, only the values where the difference in elevation was positive were used to calculate the amount of sedimentation, denoted as V. A comparison of the relationship between H/L and V, with and without the countermeasure and by arrangement distance, is shown in Figure 23.

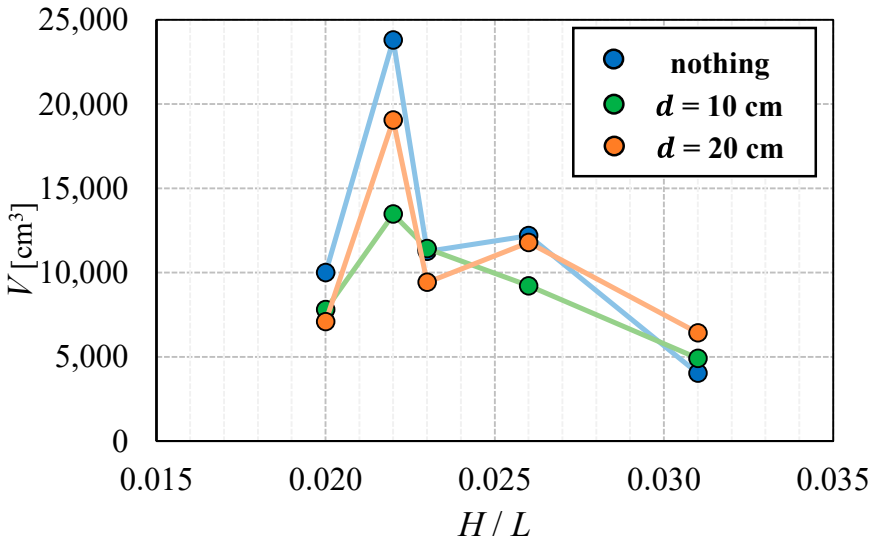


Figure 23. Relationship between wave steepness and amount of sediment.

Figure 23 reveals that under wave conditions where H/L is less than 0.026, the installation of the staggered piles effectively reduces the amount of sedimentation in the land area to levels equal to or lower than those observed in scenarios without the countermeasure. Notably, under the wave condition of H/L = 0.022, Figure 11a indicates that the landform change without countermeasure is significant, leading to considerable gravel deposition in the land area. Under conditions with extensive landform change, such as berm formation, the staggered piles significantly inhibit gravel run-up. Meanwhile, under wave conditions with an H/L of 0.031, the amount of sedimentation in the land area increased compared to cases without the countermeasure, regardless of the pile-row installation interval. The larger the H/L value, the smaller the amount of gravel transported by breaking waves. Therefore, the gravel transported by upwelling waves can easily pass through plies. The staggered piles reduced the flow volume and increased the velocity of the gravel passing through piles, which resulted in the gravel being transported further to the shore side.

The continuous piles effectively suppress the accumulation of gravel in the land area for waves with a small H/L, independent of the distance between pile rows. However, for waves with a large H/L, it enhances sedimentation. In this study, the pile row spacing should be reduced to 10 cm rather than 20 cm to complicate the gravel run-up path.

7. Conclusions

In this study, staggered piles' placement as a countermeasure against river mouth closure and the effect on gravel beaches under various wave conditions were investigated by hydraulic model experiments. The topographic change with and without a staggered arrangement of piles and the changes when the distance of the pile rows in the offshore direction was altered were compared. Based on the effectiveness of the three countermea-

sures, the conditions for installing an effective river mouth closure countermeasure were investigated. The main conclusions are as follows:

1. The staggered piles near the shoreline significantly influence the process of topographic change over time, and shorter distances between pile rows enhance the control of berm development.
2. The staggered arrangement was found to be effective in reducing the maximum height of the berm for waves with a small H/L. Under wave conditions with an $H/L = 0.022$, the reduction was about twice as large. For waves with a large H/L, shorter distances between pile rows proved to be more effective in lowering the maximum height of the berm.
3. The staggered arrangement was also effective in advancing the maximum elevation of the berm offshore under all wave conditions. The movement of 5 cm to 10 cm toward the shore was observed at the maximum elevation. Furthermore, the installation of staggered piles altered the shape of the berm.
4. The staggered piling arrangement effectively suppressed the accumulation of gravel in the land area for waves with a small H/L, regardless of the distance between the piles. The amount of land gravel sedimentation could be reduced by up to 57%. To maintain the complexity of the channel, the distance between the piles should be kept short.

The effectiveness of the staggered piles installed on the gravel beach was confirmed under a variety of wave conditions. In addition, the effectiveness of the staggered piles changed depending on the wave conditions and the pile spacing, and it also influenced the landform change process.

The proposal in this study will replace the manual excavation work with the installation of the piling structure to prevent closure. It is expected to reduce the number of personnel required for excavation work and to establish the coastal and river management system linked to a remote monitoring system. The shapes of river mouths connecting to the coast vary widely. When installing the staggered piles, general versatility and practicality should be clarified, such as the study of the layout form assuming the specific shape of the river mouth and the effectiveness of the staggered piles when the bottom material is sand. In addition to steel pipe piles, wooden piles are also considered to be useful in terms of the environment and landscape. As concrete materials are exposed to seawater, it is important to consider measures to prevent salt damage. It is necessary to investigate whether the same effect can be obtained for other materials in the future. It is also necessary to explore methods of installing piles and preventing corrosion and rusting based on the long-term operation of the countermeasure. Currently, piles for offshore civil engineering are in widespread use. Piles suitable for use under seawater should be used because piles with seawater and salt-resistant specifications are used at offshore civil engineering sites, where the steel bars used have been treated to prevent corrosion. Once the effectiveness of the installed piles is demonstrated, it is believed that a continuous effect can be obtained by gradually moving the piles offshore. The use of monopile-type foundations, which are used in offshore wind power generation, is considered to provide the easiest installation and movement of the pile installation location.

Further studies are needed for their practical application. The hydraulic experiments in this study did not measure flow velocities. The effects of changes in the wave field on the movement of gravels and topographic change have not yet been clarified. In the future, studying the influence of the countermeasure on the topography based on the changes in the flow velocity field caused by the different installation conditions of the staggered piles using numerical computation is also necessary.

Author Contributions: Conceptualization, N.M.; methodology, Y.T. and M.K.; software, Y.T. and M.K.; validation, Y.T. and M.K.; formal analysis, Y.T.; investigation, Y.T.; resources, Y.T.; data curation, Y.T. and M.K.; writing—original draft preparation, Y.T.; writing—review and editing, M.K., N.M. and T.N.; visualization, Y.T.; supervision, M.K.; project administration, M.K.; funding acquisition, M.K. All authors have read and agreed to the published version of the manuscript.

Funding: This research received no external funding.

Institutional Review Board Statement: Not applicable.

Informed Consent Statement: Not applicable.

Data Availability Statement: The original contributions presented in this study are included in the article. Further inquiries can be directed to the corresponding author.

Conflicts of Interest: The authors declare no conflicts of interest.

References

1. Tonis, I.E.; Stam, J.M.T.; Graaf, J. Morphological changes of the Haringvliet estuary after closure in 1970. *Coast. Eng.* **2002**, *44*, 191–203. [CrossRef]
2. Roca, M.; Navarro, G.; Garcia-Sanabria, J.; Caballero, I. Monitoring sand spit variability using Sentinel-2 and Google Earth Engine in a Mediterranean estuary. *Remote Sens.* **2022**, *14*, 2345. [CrossRef]
3. Becker, A.; Laurenson, L.J.B.; Bishop, K. Artificial mouth opening fosters anoxic conditions that kill small estuarine fish. *Estuar. Coast. Shelf Sci.* **2009**, *82*, 566–572. [CrossRef]
4. Behrens, D.K.; Bombardelli, F.A.; Largier, J.L.; Twohy, E. Characterization of time and spatial scales of a migrating rivermouth. *Geophys. Res. Lett.* **2009**, *36*, L09402. [CrossRef]
5. Ranasinghe, R.; Pattiaratchi, C.; Masselink, G. A morphodynamic model to simulate the seasonal closure of tidal inlets. *Coast. Eng.* **1999**, *37*, 1–36. [CrossRef]
6. Nurfaida, W.; Sato, S. A study on hydrodynamic characteristics and resulting morphological formation of sand spit around the Tenryu River mouth based on image analysis. *Procedia Eng.* **2015**, *116*, 141–148. [CrossRef]
7. Li, J.; Fuhrman, D.R.; Kong, X.; Xie, M.; Yang, Y. Three-dimensional numerical simulation of wave-induced scour around a pile on a sloping beach. *Ocean Eng.* **2021**, *233*, 109174. [CrossRef]
8. Barrie, A.; Wang, C.; Liang, F.; Qi, W. Experimental investigation on the mechanism of local scour around a cylindrical coastal pile foundation considering sloping bed conditions. *Ocean Eng.* **2024**, *312*, 119225. [CrossRef]
9. Mamoon, A.; Zhao, M.; Wu, H.; Keshavarzi, A. Experimental investigation of local scour around two submerged short square piles under tandem, side-by-side and staggered arrangements in steady current. *Ocean Eng.* **2022**, *261*, 112156. [CrossRef]
10. Liu, M.; Wang, H.; Tang, G.; Shao, F.; Jin, X. Investigation of local scour around two vertical piles by using numerical method. *Ocean Eng.* **2022**, *244*, 110405. [CrossRef]
11. Anand, A.; Beg, M. Local scour at group of bridge piers founded in gravel bed in staggered arrangement. *Results Eng.* **2024**, *23*, 102608. [CrossRef]
12. Torii, Y.; Kiku, M. Development of 3d topographic measurement method to capture topographic changes over time during hydraulic model experiments and investigation of its usefulness. *Jpn. J. JSCE* **2023**, *79*, 23-18023. [CrossRef]
13. Masselink, G.; Turner, I.L. Large-scale laboratory investigation into the effect of varying back-barrier lagoon water levels on gravel beach morphology and swash zone sediment transport. *Coast. Eng.* **2012**, *63*, 23–38. [CrossRef]

Disclaimer/Publisher's Note: The statements, opinions and data contained in all publications are solely those of the individual author(s) and contributor(s) and not of MDPI and/or the editor(s). MDPI and/or the editor(s) disclaim responsibility for any injury to people or property resulting from any ideas, methods, instructions or products referred to in the content.